• Basic Research •

Exosome-mediated aptamer S58 reduces fibrosis in a rat glaucoma filtration surgery model

Qian-Yi Lin[1], Xiang-Ji Li[1], Yu Leng[1], Xiao-Min Zhu[1], Min Tang[1], Yi Lin[1], Wang-Du Luo[1], Bing-Cai Jiang[1], Xia Chen[2], Lin Xie[1]

[1]Department of Ophthalmology, The Third Affiliated Hospital of Chongqing Medical University, Chongqing 401120, China

[2]Department of Ophthalmology, Daping Hospital of Army Medical University, Chongqing 400042, China

Correspondence to: Lin Xie. Department of Ophthalmology, The Third Affiliated Hospital of Chongqing Medical University, 1 Shuanghu Road, Chongqing 401120, China. xielin@hospital.cqmu.edu.cn

Received: 2021-11-19 Accepted: 2022-02-21

Abstract

● **AIM:** To confirm whether exosome-mediated delivery of aptamer S58 (Exo-S58) has a better antifibrotic effect than naked S58 in human conjunctival fibroblasts (HConFs) and a rat glaucoma filtration surgery (GFS) model.

● **METHODS:** To enhance the effective reaction time of aptamer S58 *in vivo*, we loaded aptamer S58 into exosomes derived from HEK293T cells by PEI transfection to determine the effect of Exo-S58 in HConFs and a rat GFS model.

● **RESULTS:** Exo-S58 can significantly reduce cell proliferation, migration and fibrosis in TGF-β2-induced HConFs. In an *in vivo* experiment, Exo-S58 treatment prolonged filtering bleb retention and reduced fibrosis compared with naked S58 treatment in GFS rats.

● **CONCLUSION:** The exosomes are safe and valid carriers to deliver aptamers. Furthermore, Exo-S58 exhibited superior antifibrotic effect than naked S58 both in HConFs cells and rat GFS models.

● **KEYWORDS:** nanomedicine; exosomes; aptamer; drug delivery; glaucoma surgery; transforming growth factor-beta; anti-fibrosis

DOI:10.18240/ijo.2022.05.02

Citation: Lin QY, Li XJ, Leng Y, Zhu XM, Tang M, Lin Y, Luo WD, Jiang BC, Chen X, Xie L. Exosome-mediated aptamer S58 reduces fibrosis in a rat glaucoma filtration surgery model. *Int J Ophthalmol* 2022;15(5):690-700

INTRODUCTION

Glaucoma is recognized as an irreversible progressive neurodegenerative eye disease that can cause optic atrophy, visual field defects and blindness[1-3]. According to previous studies, glaucoma is also a multifactorial disease accompanied by pathologically elevated intraocular pressure (IOP) as the most important risk factor[4-6]. As such, glaucoma filtration surgery (GFS) has been an integral part of glaucoma control strategies through drainage of the aqueous humour to decrease IOP[7-9]. However, surgical failure may occur because of excessive subconjunctival fibrosis and scar formation caused by wound vascular reaction, exudate stimulation and hormones[10-12]. Mitomycin C (MMC) and 5-fluorouracil (5-FU) have been generally used to avoid unexpected filtering bleb fibrosis in clinical practice and have side effects such as bleb leakage, endophthalmitis and corneal epithelial toxicity[13-15]. Therefore, it is necessary to identify safe and effective antifibrotic alternatives that can be used to prevent scar formation and preserve filtering bleb function after GFS.

Previous reports have demonstrated that transforming growth factor-β (TGF-β) ligands play a crucial role in cell proliferation, migration, conjunctival scarring and wound healing[16-17]. As one of the identified TGF-β isoforms, TGF-β_2 is closely related to the process of conjunctival scarring and fibrosis[18-19]. Consequently, TGF-β ligands or receptors are therapeutic targets in the process of postoperative fibrosis through antibody neutralization[20-21], proteoglycan-like decorin inactivation and blockage of exogenous receptors[22-23].

Aptamers are single-stranded DNA (ssDNA) or RNA oligonucleotides that can bind to a target protein[24-25] and are characterized by low toxicity[26], high selectivity and binding affinity[27]. In our previous study, we applied systematic evolution of ligands by exponential enrichment (SELEX) to identify and synthesize the DNA aptamer S58, which could bind to TGF-β receptor II (TβRII) with high affinity. Experiments *in vitro* and *in vivo* proved that aptamer S58 could reduce TGF-β_2-induced fibrosis, and fewer myofibroblasts were observed in the S58 group compared with MMC groups[28-29]. However, the aptamer's effective reaction time was limited by nuclease degradation. Thus, it deserves advanced investigation

to determine whether a nontoxic and protective delivery vector can preserve the efficacy of aptamer S58.

Recently, exosome drug delivery systems have received great attention due to their high delivery efficiency, long circulation times and great biocompatibility[30-33]. Furthermore, exosomes have multiple advantages compared to viruses and existing synthetic carrier systems in terms of immunogenicity, blood stability and tissue penetration[33]. Several studies have shown that exosomes carrying short interfering ribonucleic acid (siRNA) sequences could access target tissues for drug delivery[33-35].

In this study, we loaded S58 into exosomes (Exo-S58) and confirmed whether Exo-S58 has a better antifibrotic effect than naked S58 in human conjunctival fibroblast (HConF) cells and in rat GFS models.

MATERIALS AND METHODS

Ethical Approval Animal experiments were approved by the Animal Ethics Committee of Chongqing Medical University. All animal procedures complied with the ARVO Statement for the Use of Animals in Ophthalmic and Visual Research.

Cell Culture and Treatment The human embryonic kidney cell line HEK293T was cultured in complete medium containing 10% exosome-free foetal bovine serum (FBS; Biological Industries, Kibbutz Beit Haemek, Israel), Dulbecco's modified Eagle's medium (DMEM; Biological Industries), and 1% cyan-streptomycin (Biological Industries) at 37℃ and 5% CO_2. Primary HConFs were cultured in complete medium containing 10% FBS, DMEM and 1% cyan-streptomycin at 37℃ and 5% CO_2. In the S58 treatment group, aptamer S58 was first diluted in ddH_2O to a final concentration of 50 nmol/L. Exosomes (3.75 μg) loaded with 50 nmol/L S58 were used in the Exo-S58 treatment group. For exosome treatment, 3.75 μg of unloaded exosomes were used. TGF-β_2 (5 ng/mL, PeproTech, Rocky Hill, NJ, USA) was used for all cell experiments.

Isolation and Characterization of Exosomes HEK293T cell culture medium was obtained every other day followed by centrifugation at 300×g for 10min and 2000×g for 10min. After further centrifugation at 10 000×g for 45min, the supernatant was filtered through a 0.22-μm filter membrane. Exosome pellets can be obtained through two runs of ultracentrifugation (CP100MX, Hitachi, Japan) at 100 000×g for 70min[36]. The collected pellets were resuspended in phosphate-buffered saline (PBS) and stored at -80℃ for further use.

For the transmission electron microscopy (TEM) assay, exosome pellets were added to copper grids for fixation. A 2% uranyl acetate solution was then put on grids for 5min at room temperature. Images were taken by an electron microscope (HT7700, Hitachi, Japan) after the grids were washed and dried. Nano flow cytometry (NanoFCM; Fujian, China) was employed to measure the size distribution of the exosome pellets[37]. The expression level of marker proteins of purified exosomes was detected by Western blot containing the primary antibodies rabbit anti-CD63 (ab134045, Abcam, Cambridge, MA, USA), rabbit anti-CD81 (ab109201, Abcam), and rabbit anti-TSG101 (ab125011, Abcam).

Aptamer S58 Loading For aptamer loading, 7.5 μg of exosomes was incubated with the aptamer mixture after a 20-min incubation of 100 nmol/L S58 (Sangon Biotech, Shanghai, China) and 1 mg/mL polyethyleneimine (PEI) in Hepes buffered saline (HBS) according to the PEI-transferrinfection kit protocol (Thermo Scientific, Carlsbad, MA, USA). Ultracentrifugation at 100 000×g for 90min was performed to remove the redundant aptamers and PEI after incubation at 4℃. The resulting pellet was rinsed and then resuspended in PBS. Nano flow cytometry was applied to measure the loading efficiency of aptamer S58.

Exosomal Staining Exosomes were stained with a PKH26 red fluorescent cell labelling kit (Ur52302, Umibio, Shanghai, China) according to the manufacturer's protocol[38]. In brief, the PKH26 linker was diluted with 100 μmol/L Diluent C. Then, 10 μg of exosomes was added to 50 μL of dye solution and mixed by pipetting for 1min. After 10min of incubation at 37℃, the staining solution was resuspended in 10 mL of PBS. Ultracentrifugation at 100 000×g for 90min was performed to remove redundant dye at 4℃. The exosomes were resuspended in PBS for further use. The fluorescence intensity of PKH26-labelled exosomes was detected by confocal microscopy.

Cell Cytotoxicity Assay HConFs were seeded into 96-well plates at a density of 4×10^3 cells per well and cultured in 200 μL of fresh complete medium with different treatments for 24, 48, and 72h. Cell cytotoxicity was detected with an LDH cytotoxicity assay kit (C0017, Beyotime, Shanghai, China). Twelve microlitres of LDH release reagent was added per well and incubated with cells for 1h. After centrifugation at 400×g for 5min, 120 μL of supernatant from each well was collected in new 96-well plates. The absorbance values at 490 nm of each well were determined by Multiscan Spectrum (BioTek, Winooski, VT, USA), and the LDH release rate was statistically evaluated.

Cell Viability Assay HConFs were plated into 96-well plates at a density of 4×10^3 cells per well and cultured in 100 μL of fresh complete medium with different treatments for 24, 48, and 72h. Ten microlitres of CCK-8 reagent (Biosharp, Beijing, China) were added per well and incubated with the cells for 2h. The absorbance values at 450 nm of each well were identified by Multiscan Spectrum (BioTek), and the cell viability rate was statistically analysed.

Immunofluorescence Microscopy HConFs were plated into 24-well plates at a density of 1×10^4 cells per well and treated with PKH26-labelled exosomes loaded with Alexa 488-labelled S58. The cells were rinsed and fixed with 4%

paraformaldehyde solution for 15min at room temperature immediately after permeabilization with 0.1% Triton X-100 for 15min and blocking with 1% bovine serum albumin (BSA) for 1h at room temperature. 4',6-diamidino-2-phenylindole (DAPI) staining was performed for 10 min. Images were taken by an inverted fluorescence microscope (Ti2-U, Nikon, Japan) and analysed.

Cell Migration Assay HConFs were plated at a density of 4×10^3 cells per well and cultured in 100 μL of serum-free medium in 24-well migration chambers. Then, 600 μL of fresh complete medium with 20% FBS was added below the chambers. Cell medium was removed from the chambers after cells were incubated with different treatments for 24h at 37℃. Then, the cells were fixed and stained with crystal violet for 15min at room temperature followed by three washes with PBS. Photographs were taken by an inverted microscope (Nikon).

Western Blot Isolated HConFs and exosomes were lysed for 40min on ice with radioimmunoprecipitation (RIPA) buffer (Beyotime) containing protease inhibitors (Thermo Scientific, IL, USA). The supernatant was extracted after centrifugation at 12 000×g for 15min, and a bicinchoninic acid kit (BCA; Beyotime) was used to quantify the protein according to the manufacturer's protocol. The extracted samples were separated by 6%-15% SDS-polyacrylamide gel electrophoresis (PAGE) and transferred onto a polyvinylidene fluoride (PVDF) membrane (Millipore, Billerica, MA, USA). Following blocking in Western blocking buffer (Beyotime) for 1h, membranes were incubated with primary antibodies including rabbit anti-collagen I (ab260043, Abcam), rabbit anti-vimentin (ab92547, Abcam), mouse anti-α-SMA (ab7817, Abcam), rabbit anti-fibronectin (ab268020, Abcam), rabbit anti-CD63 (ab134045, Abcam), rabbit anti-CD81 (ab109201, Abcam), rabbit anti-TSG101 (ab125011, Abcam) and mouse anti-GAPDH (AG019, Beyotime, China) overnight at 4℃. After rinsing three times with Tris-buffered saline Tween (TBST) for 10min, the protein membranes were incubated with the specific HRP-linked secondary antibody for 1h at room temperature. The protein membranes were visualized with a gel imaging analysis system (Bio-Rad, Hercules, CA, USA).

Experimental Animals and Treatment Totally 24 Adult male Sprague-Dawley rats that weighed 200-300 g were purchased from the Laboratory Animal Center of Chongqing Medical University. The rats were anaesthetised by an intraperitoneal injection of 5 mL/kg 7% chloral hydrate (Sangon Biotech) followed by ocular surface anaesthesia using 0.5% oxybuprocaine hydrochloride eye drops (Santen Pharmaceutical Co., Ltd. Osaka, Japan). GFS in the rats was performed on bilateral eyes based on a previous technique[39]. Then, the rats were treated with subconjunctival injection containing saline, S58 (50 nmol/L) or Exo-S58 (3.75 μg) randomly every other week after surgery (n=6/group). The effects of different interventions against scar formation through subconjunctival injection were evaluated at days 0, 7, and 14. Additionally, rats operated eyes were tested and evaluated for IOP and filtering bleb using a slit lamp (CARL ZEISS, Germany) and tenonometer (TonoPen; Medtronic Solan, FL, USA), respectively, at specific times.

Histological Analysis To observe the change in scarring formation following GFS, the eyeballs from the rats were collected and fixed with 4% paraformaldehyde on postoperative day 14. After dehydration with graded ethanol, the conjunctival tissue was embedded in paraffin. Haematoxylin-eosin (HE) staining and Masson staining were used to detect the percentage of collagen after 3-μm-thick sections from the eyeballs were sliced. Furthermore, immunofluorescence staining was also performed to determine the tissue fibrosis level. Citrate acid was used to retrieve the antigen from the sections after deparaffination and rehydration. Then, 3% hydrogen peroxide was incubated with the sections in the dark for 25min. After blocking with 1% goat serum albumin for 30min, the sections were incubated with primary antibodies, including mouse anti-α-SMA (ab7817, Abcam) and rabbit anti-collagen I (ab260043, Abcam), overnight at 4℃. The sections were incubated with specific secondary antibodies for 1h and stained with DAPI for 5min. Images were captured by a fluorescence microscope (Nikon Eclipse Ti-SR, Nikon, Japan).

Statistical Analysis All values are presented as the mean±SD. Statistical analysis for comparison of multiple columns or groups was performed by one-way ANOVA using GraphPad Prism 7 (GraphPad, San Diego, CA, USA), and a P<0.05 was considered statistically significant.

RESULTS

Characterization of the Exosomes from HEK293T Cells The exosomes were purified from HEK293T cell culture medium by ultracentrifugation, and characterization of the exosomes was successfully validated by TEM, NanoFCM and Western blot. The TEM results showed that the exosome particles were integral and hemispheric with a double membrane less than 100 nm in diameter (Figure 1A). NanoFCM measured that the average diameter of exosome particles was approximately 73 nm at a concentration of 5.32×10^9/mL (Figure 1B). Western blot analysis showed that the expressions of the exosome marker proteins CD63, CD81, and TSG101 were positive (Figure 1C).

Exosomes Mediated Delivery of S58 into HConFs To improve the therapeutic effect of S58, aptamer S58 was loaded into exosomes by PEI transfection according to the protocol. After transfection, excess S58 and PEI were removed by ultracentrifugation. In addition, we determined the loading efficiency of exosome-encapsulated S58 by using NanoFCM analysis. The results of the NanoFCM analysis showed that

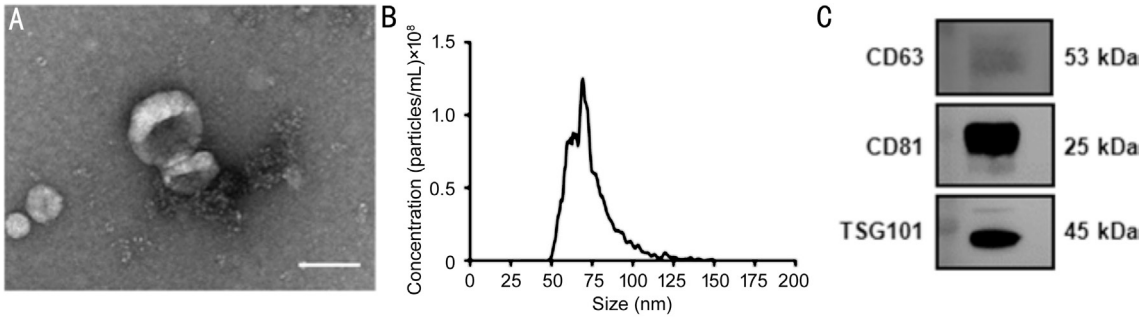

Figure 1 Characterization of exosomes A: TEM image of exosomes derived from HEK293T cells. Scale bar, 100 nm. B: NanoFCM analysis determined the average concentrations and size ranges of exosomes derived from HEK293T cells. C: Western blotting of 10 μg of protein from purified exosomes from HEK293T cells. TEM: Transmission electron microscopy; NanoFCM: Nano flow cytometry.

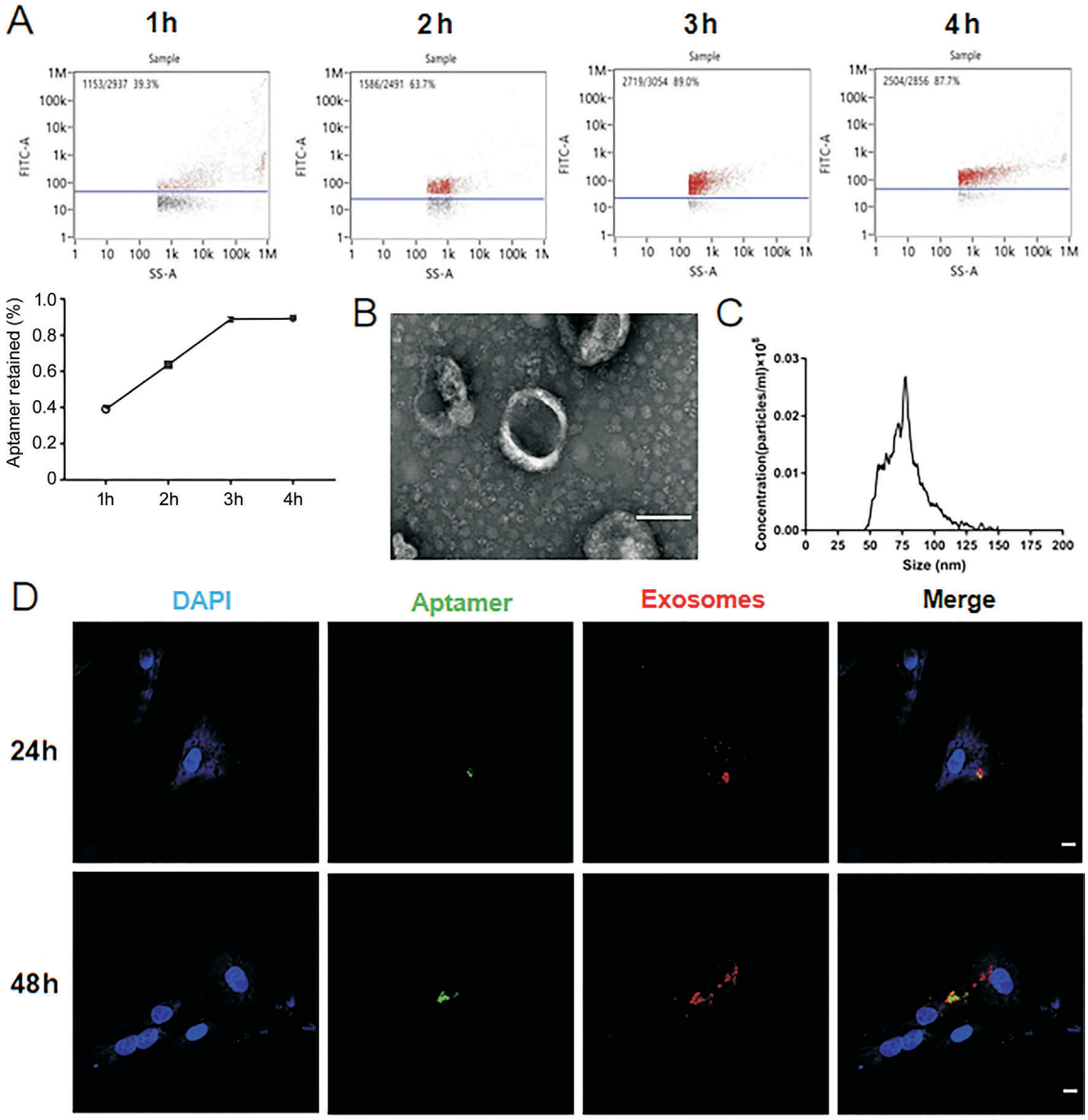

Figure 2 Characterization of Exo-S58 and uptake of Exo-S58 by HConF cells A: Aptamer S58 was incubated with exosomes for different times (1, 2, 3, and 4h). The aptamer retention rate was calculated by NanoFCM. *n*=3. B: TEM image of Exo-S58. Scale bar, 100 nm. C: NanoFCM analysis determined the average concentrations and size ranges of Exo-S58. D: Confocal microscopy images showed that HConFs could take in PKH26-labelled exosomes loaded with Alexa 488-labelled aptamer S58 at 24 and 48h. Scale bar, 10 μm. Exo-S58: Exosome-mediated delivery of aptamer S58; TEM: Transmission electron microscopy. DAPI: 4',6-diamidino-2-phenylindole.

incubation with exosomes for 3h reached the greatest aptamer retention rate at 88.83%±1.06% (Figure 2A). Furthermore, TEM showed that the morphological structure of exosomes loaded with S58 did not change after transfection with PEI

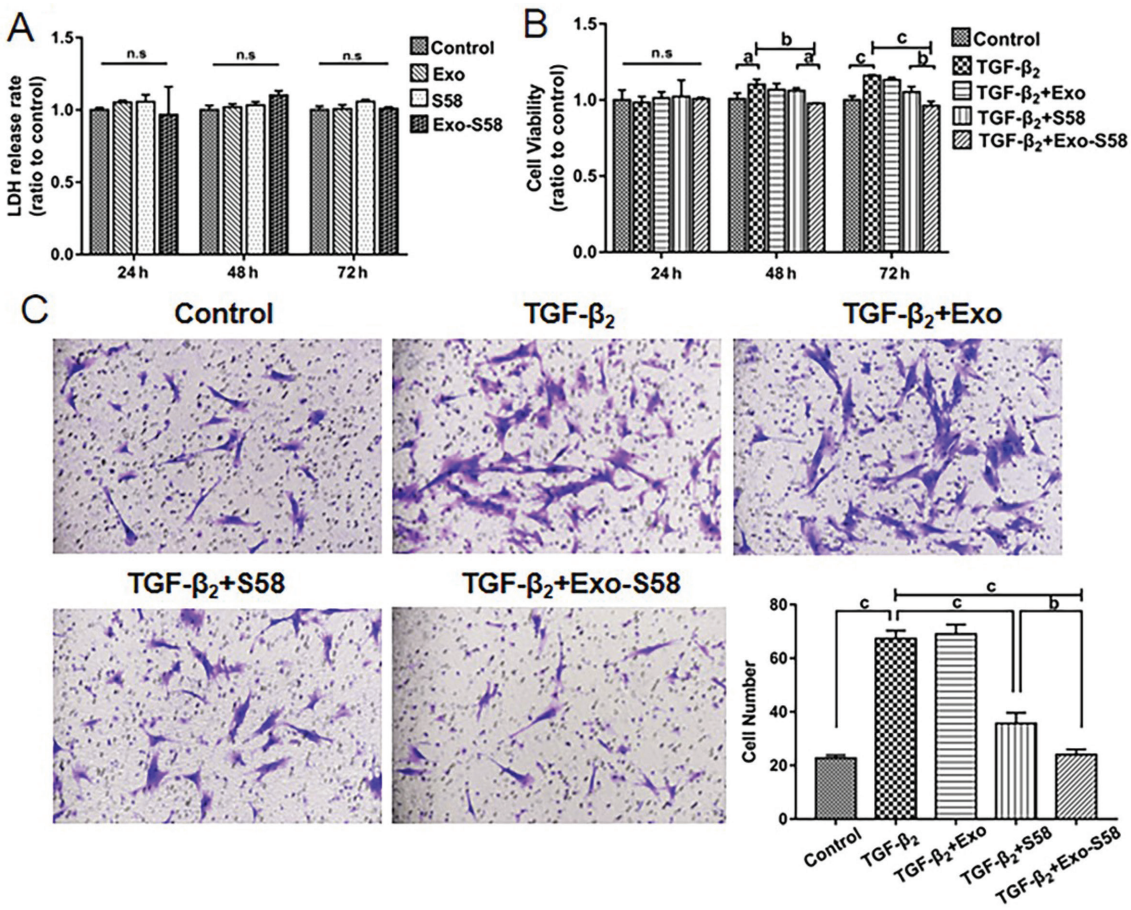

Figure 3 Effect of Exo-S58 on the cell proliferation and migration A: Exo-S58 could be taken up by HConFs cells without cytotoxity. B: CCK-8 assay was performed after HConFs were incubated with different treatment for 24, 48, and 72h. C: Representative images and quantification of cell motility were performed after HConFs were incubated with different treatments for 24h. n=6; ^{a}P<0.05; ^{b}P<0.01; ^{c}P<0.001. Exo-S58: Exosome-mediated delivery of aptamer S58; CCK-8: Cell counting kit-8.

(Figure 2B). Then, NanoFCM measured that the average diameter of loaded exosome particles was approximately 78 nm at a concentration of 1.34×10^{8}/mL (Figure 2C). Therefore, incubation with exosomes for 3h was performed to load aptamer S58. To determine whether exosomes can deliver S58 into HConFs, the fluorescence of PKH26-labelled exosomes and Alexa 488-labelled aptamer was detected after incubation with cells for 24h and 48h by confocal fluorescence imaging (Figure 2D). The confocal imaging results showed that HConFs could take up Exo-S58, and incubation with exosomes for 48h reached the highest exosome uptake efficiency.

Exo-S58 Inhibited TGF-β_2-induced HConFs Cell Proliferation and Migration Next, to investigate the cytotoxicity of Exo-S58, HConFs were incubated with different treatments for 24, 48, and 72h. The LDH release rate showed that Exo-S58 did not cause cytotoxicity to the cells (Figure 3A). To investigate the effect of Exo-S58 on HConFs cell proliferation and migration, they were cultured with different treatments. The data showed that there were no significant differences in cell viability among the different groups at 24h. TGF-β_2 significantly promoted HConFs viability, while the cell viability of the Exo-S58 group was decreased significantly compared with the naked S58 group at 48 and 72h (Figure 3B). The result also showed that TGF-β_2 treatment significantly promoted HConFs migration, while the migration of Exo-S58 treatment was decreased significantly compared with naked S58 treatment (Figure 3C). These results suggested that Exo-S58 could inhibit cell proliferation and migration caused by TGF-β_2 more effectively compared with naked S58 in HConFs.

Exo-S58 Inhibited TGF-β_2-induced HConFs Fibrosis Western blot was used to determine the antifibrotic effect of Exo-S58 after the HConFs were incubated with different treatments for 48h. The expression levels of the proteins fibronectin, collagen I, vimentin, α-SMA in the TGF-β_2 group were increased significantly, while fibrosis protein expression levels in the Exo-S58 group were decreased significantly compared with those in the naked S58 group (Figure 4). The result indicated that Exo-S58 could reduce TGF-β_2-induced fibrosis significantly in HConFs compared with naked S58.

Exo-S58 Prolonged the Bleb Survival in the Rat GFS Model The rats were treated with subconjunctival injection containing saline, S58 or Exo-S58 randomly after surgery. To

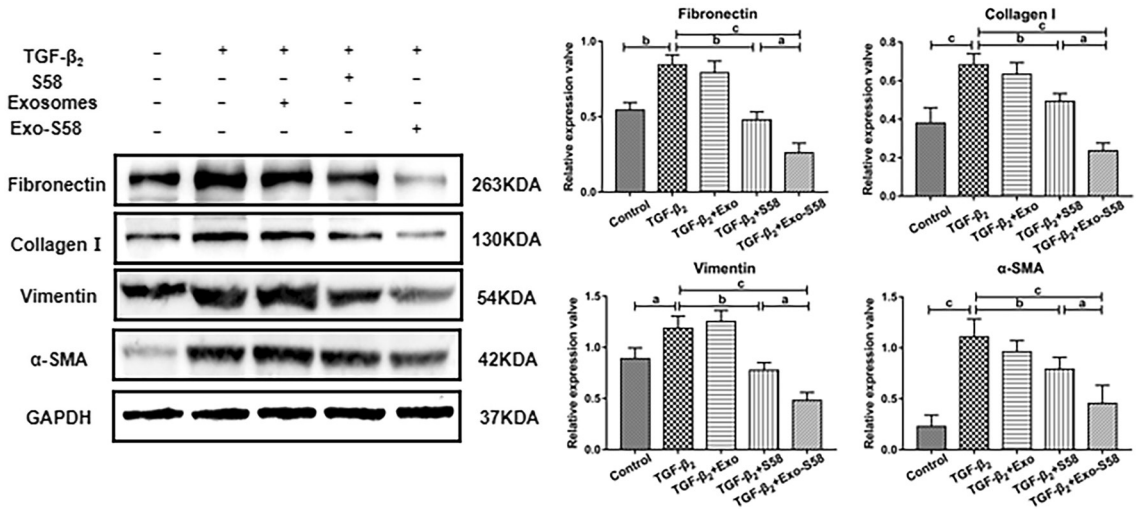

Figure 4 Western blot of fibrosis-related proteins The protein levels of fibronectin, collagen I, vimentin and α-SMA were detected by Western blotting after HConFs were incubated with different treatments for 48h. n=3; ^{a}P<0.05; ^{b}P<0.01; ^{c}P<0.001. Exo-S58: Exosome-mediated delivery of aptamer S58; α-SMA: α-smooth muscle actin; GAPDH: Glyceraldehyde-3-phosphatedehydrogenase.

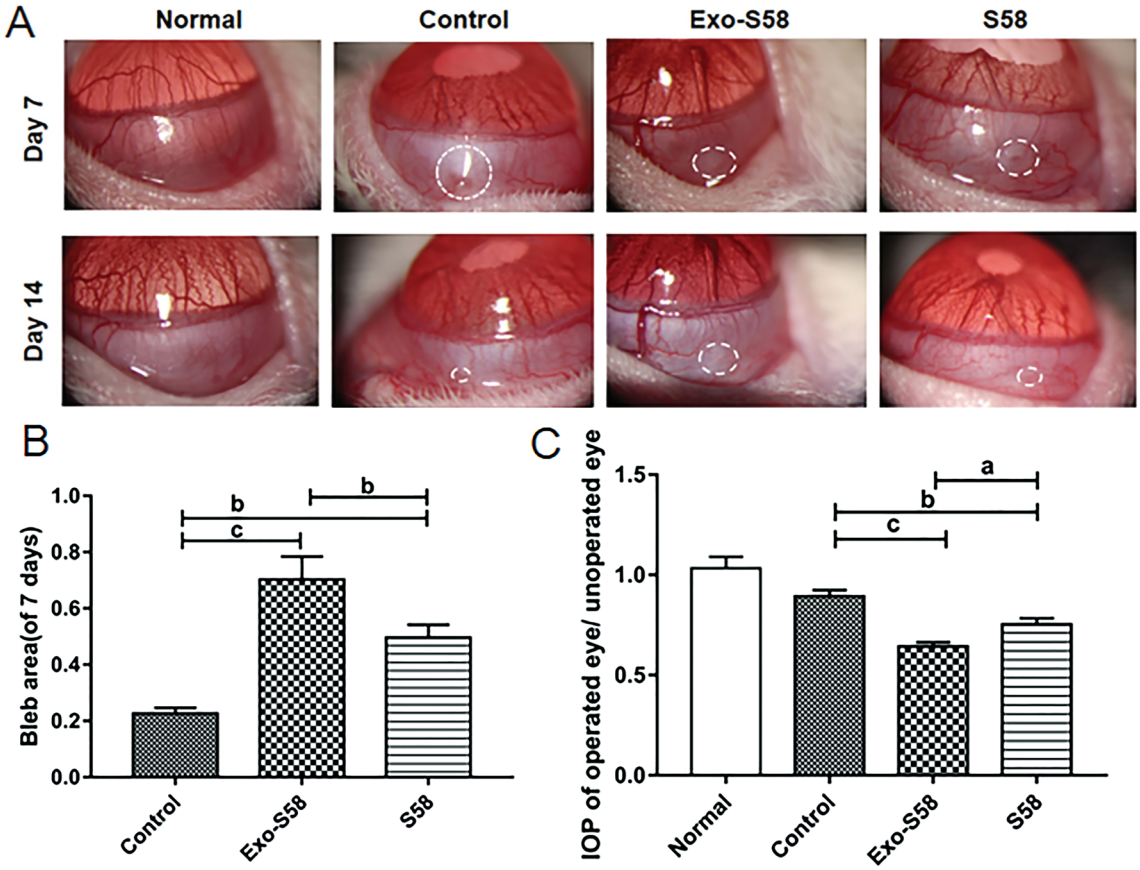

Figure 5 Exo-S58 treatment prolonged filtering blebs retention in rats GFS model A, B: Typical pictures from slit lamp showing bleb characteristics in different groups (the area of blebs is outlined and measured) at operative days 7 and 14. C: The mean IOP of the operated eyes were measured. n=6; ^{a}P<0.05; ^{b}P<0.01; ^{c}P<0.001. Exo-S58: Exosome-mediated delivery of aptamer S58; GFS: Glaucoma filtration surgery; IOP: Intraocular pressure.

better observe the change after GFS, IOP and filtering bleb areas of the rats were detected on operative days 0, 7 and 14. Results showed that the Exo-S58 and S58 treatment prolonged the filtering bleb retention significantly, while Exo-S58 treatment prolonged bleb retention more effectively than S58 treatment (Figure 5A, 5B). Statistical analysis of mean IOP in the surgical eyes showed that the IOP of rats in the Exo-S58 group was lower than that of rats in the S58 group on operative day 14, while IOP of the control group was significantly higher than that in both groups (Figure 5C).

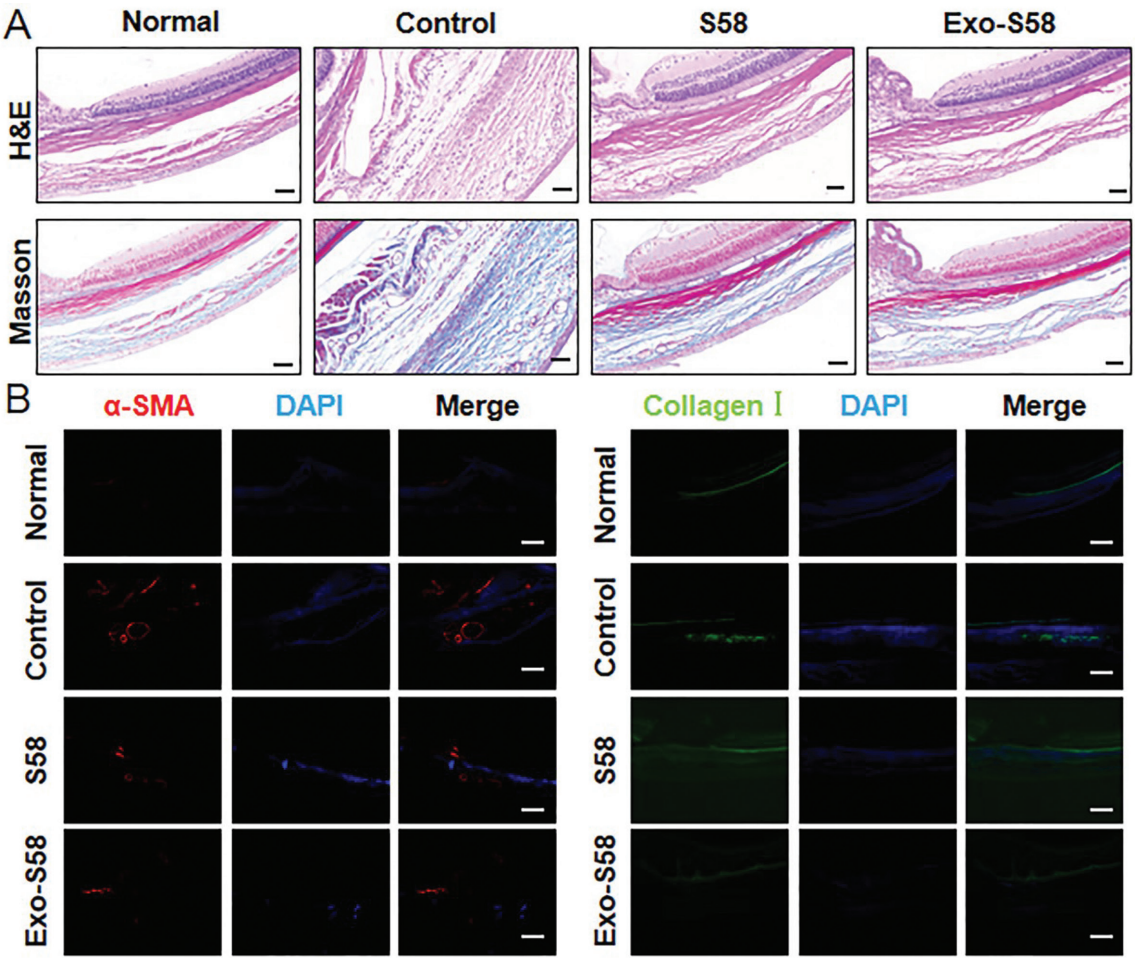

Figure 6 Histologic characteristics A: Representative HE staining and Masson staining images in the conjunctiva of rats after different treatments on postoperative day 14. Masson staining revealed collagen deposition, and the percentage of collagen deposits from different groups was measured. Scale bars: 50 μm. B: Immunofluorescence images of α-SMA and collagen I in the conjunctiva of rats after different treatments on postoperative day 14. *n*=6. Exo-S58: Exosome-mediated delivery of aptamer S58; HE staining: Haematoxylin-eosin staining; α-SMA: α-smooth muscle actin; DAPI: 4',6-diamidino-2-phenylindole.

Histologic Characteristics of Filtering Blebs Rats from different groups were sacrificed on operative day 14. HE staining, Masson staining and immunofluorescence staining were performed on the sections to observe the pathological changes. Representative Masson staining images of sections showed that the control group had more collagen deposition in the surgical site than the Exo-S58 group and S58 group, while the Exo-S58 group exhibited significantly less collagen deposition than the S58 group (Figure 6A). Immunofluorescence staining showed that the expression of collagen-I and α-SMA in the control group was higher than that in the Exo-S58 group and S58 group, while Exo-S58 significantly decreased fibrosis protein expression relative to that in the S58 group (Figure 6B). The above results indicated that Exo-S58 reduces fibrosis in rats after GFS.

DISCUSSION

GFS is an effective therapeutic strategy for glaucoma[40]. The aqueous humor can be drained through the subconjunctival outflow channel, which is established through filtration surgery. However, excessive postoperative subconjunctival fibrosis would often reduce aqueous humor drainage and even lead to surgery failure[12]. MMC and 5-FU are widely used in the clinic to prevent subconjunctival excessive fibrosis, accompanied by many side effects such as bleb leakage, endophthalmitis and corneal epithelial toxicity[13-15]. A key molecule in fibrosis development is TGF-β, which accelerates cell differentiation, migration, and proliferation[41]. As one of the identified TGF-β isoforms, TGF-β_2 is closely related to the process of conjunctival scarring and fibrosis[18-19]. To inhibit TGF-β_2 stimulation, we developed aptamer S58 to specifically bind to TβRII. Based on the conformational flexibility and targeting specificity, aptamers can be considered as alternatives to an antibody to inhibit protein-protein interactions[42]. Although we have proved that aptamer S58 could reduce TGF-β_2-induced fibrosis *in vitro* and *in vivo*[28-29], the valid time of naked S58 is limited by several factors. Naked, single-stranded RNA could easily suffer from nuclease degradation and have poor circulation time[43]. The process of wound healing is

long lasting. Therefore, it is necessary to identify a new drug delivery system to prolong or enhance the effect of aptamer S58 for successful application to the conjunctiva after GFS.

Nano-carrier drug delivery systems can significantly improve bioavailability and efficacy of the drug in the eye. Chitosan nanomicelles carrying dexamethasone exhibited good ocular tolerance and provided a relatively longer retention time[44]. Liposomes containing betaxolol hydrochloride were more efficient than the betaxolol hydrochloride solution on decreasing IOP in rabbits[45]. For RNA drug delivery, viral vectors[46], cationic polymers[47], liposomes[48] and exosomes[33] have been used. Among all the nano-based drug delivery systems, liposomes as the most common and extensively studied vehicle that have shown therapeutic potential in many biomedical areas[49]. Despite liposomes having the advantages of biocompatibility, bio-degradability and low toxicity[50], there are many limitations, including rapid clearance of liposomes, low targeting efficiency and potential immunogenicity[49,51-52]. Exosomes as the natural carrier possess some advantages over liposomes and polymeric nanoparticles in active targeting and any immunogenicity[52-53]. Exosomes are cell-derived nanosized membrane vesicles, which transfer their components such as proteins, RNA, and DNA to mediate cell-to-cell communication[54-55]. Exosome natural biological properties contribute to high targeting efficiency, cell adhesion, cell fusion and cellular delivery of cargo[32]. Exosomes have been suggested as novel nanomaterials for treating fibrosis related diseases. Recent study explored that exosomes isolated from human umbilical cord-derived mesenchymal stem cell inhibited subretinal fibrosis by delivering miR-27b[56]. Guiot *et al*[57] suggested that macrophage-derived exosomes may reduce pulmonary fibrosis progression *via* the delivery of antifibrotic miR-142-3p. Similarly, miRNA-loaded human peripheral blood derived-exosomes may be used as a therapeutic tool to prevent cardiac fibrosis[58]. However, research about the application of exosomes on excessive subconjunctival fibrosis after GFS is lacking. Thus, we used exosomes to deliver the aptamer S58 in our study and to identify whether it would enhance or prolong the effect of the naked aptamer.

Our research suggests that Exo-S58 could reduce excessive fibrosis more effectively than naked S58 in HConF cells and in rat GFS models. Recent studies have employed exosomes purified from HEK293T cells as a new method for the *in vivo* delivery of siRNA[59-60]. In this study, we used exosomes derived from HEK293T cells to deliver aptamer S58. The obtained exosomes showed normal morphological characteristics by TEM, and aptamer S58 was loaded into exosomes by transfection efficiently without cytotoxicity. Furthermore, it was verified that Exo-S58 could be taken up by HConFs. In the HConFs treated with Exo-S58, cell proliferation, migration and the expression of fibrosis marker proteins were decreased significantly compared with those in the S58 group. In GFS rats subjected to subconjunctival injection of Exo-S58, Exo-S58 treatment prolonged filtering bleb retention and reduced the mean IOP compared with naked S58 treatment. The results of Masson staining and immunofluorescence staining indicated that Exo-S58 treatment significantly reduced fibrosis compared with S58 treatment. The loosely organized subconjunctival matrix in Exo-S58 treated eyes may contribute to the prolonged retention time of filtering blebs. Taken together, our study demonstrated that exosomes are safe and valid carriers to deliver aptamers, and Exo-S58 reduced excessive fibrosis in HConFs and in rat GFS models more effectively than naked S58. Our results are consistent with previous studies which suggested that anticancer drugs encapsulated in exosomes demonstrated enhanced anticancer properties *in vivo* compared to free drugs[61]. We suppose that the exosome membrane's lipid bilayer structure can protect the aptamer from degradation caused by direct contact with ribonuclease. It is also possible that exosomes as natural carriers yield a longer circulation and a reduced clearance rate increasing the circulation time of aptamer S58 without toxicity. In addition, exosomes may be internalized through interaction with the plasma membrane[62-65]. Indeed, there exists another hypothesis that exosomes can fuse with endosomal membranes[54,66]. As a result, exosomes loaded with aptamers S58 could easily be taken up by HConFs and improve the antifibrotic effect in the process. However, there were several limitations in our study. Although exosome-mediated S58 delivery in our study did not show obvious side effects and demonstrated the expected therapeutic effect, the possible impact of other cell-derived exosomes will need to be further studied and explained. Finally, the combination of exosomes and sustained-release material such as chitosan hydrogel may contribute to treating patients for long periods of time. Further studies are required to improve exosomes as drug carriers and the application of aptamer S58.

In conclusion, the study presents the evidence that exosomes are safe and valid carriers to deliver the aptamer S58. The exosome-mediated delivery of aptamer S58 can significantly reduce cell proliferation, migration and fibrosis in TGF-β_2-induced HConFs. Moreover, the exosome-mediated delivery of aptamer S58 exhibited superior antifibrotic effect compared to naked aptamer S58 in rat GFS models. The current study provided the possible therapeutic value for preventing scar tissue formation after GFS and other tissue fibrosis.

ACKNOWLEDGEMENTS

Authors' contributions: Lin QY designed the study, performed experiments, interpreted the data, and wrote the

manuscript. Xie L participated in foundation acquisition, planning experiments and revising the manuscript. Li XJ, Leng Y and Zhu XM conceived and performed the animal experiments. Tang M, Lin Y participated in experiments plan, and manuscript writing. Luo WD, Jiang BC and Chen X supplied materials and assisted experiments. All authors discussed the results and critically reviewed the manuscript.

Foundations: Supported by the National Natural Science Foundation of China (No.81700836; No.81470629; No.81670860); Chongqing Natural Research Foundation (No. cstc 2018jcyjAX0034).

Conflicts of Interest: Lin QY, None; **Li XJ,** None; **Leng Y,** None; **Zhu XM,** None; **Tang M,** None; **Lin Y,** None; **Luo WD,** None; **Jiang BC,** None; **Chen X**, None; **Xie L**, None.

REFERENCES

1 Flaxman SR, Bourne RRA, Resnikoff S, Ackland P, Braithwaite T, Cicinelli MV, Das A, Jonas JB, Keeffe J, Kempen JH, Leasher J, Limburg H, Naidoo K, Pesudovs K, Silvester A, Stevens GA, Tahhan N, Wong TY, Zheng YF. Global causes of blindness and distance vision impairment 1990-2020:a systematic review and meta-analysis. *Lancet Glob Heal* 2017;5(12):e1221-e1234.

2 Balendra SI, Shah PA, Jain M, Grzybowski A, Cordeiro MF. Glaucoma: hot topics in pharmacology. *Curr Pharm Des* 2017;23(4):596-607.

3 Williams PA, Marsh-Armstrong N, Howell GR; Lasker/IRRF Initiative on Astrocytes and Glaucomatous Neurodegeneration Participants. Neuroinflammation in glaucoma: A new opportunity. *Exp Eye Res* 2017;157:20-27.

4 Jonas JB, Aung T, Bourne RR, Bron AM, Ritch R, Panda-Jonas S. Glaucoma. *Lancet* 2017;390(10108):2183-2193.

5 Chan TCW, Bala C, Siu A, Wan F, White A. Risk factors for rapid glaucoma disease progression. *Am J Ophthalmol* 2017;180:151-157.

6 McMonnies CW. Glaucoma history and risk factors. *J Optom* 2017;10(2):71-78.

7 Shah M. Micro-invasive glaucoma surgery - an interventional glaucoma revolution. *Eye Vis* (*Lond*) 2019;6:29.

8 Gazzard G, Konstantakopoulou E, Garway-Heath D, Garg A, Vickerstaff V, Hunter R, Ambler G, Bunce C, Wormald R, Nathwani N, Barton K, Rubin G, Buszewicz M, LiGHT Trial Study Group. Selective laser trabeculoplasty versus eye drops for first-line treatment of ocular hypertension and glaucoma (LiGHT):a multicentre randomised controlled trial. *Lancet* 2019;393(10180):1505-1516.

9 Lusthaus J, Goldberg I. Current management of glaucoma. *Med J Aust* 2019;210(4):180-187.

10 Zada M, Pattamatta U, White A. Modulation of fibroblasts in conjunctival wound healing. *Ophthalmology* 2018;125(2):179-192.

11 Addicks EM, Quigley HA, Green WR, Robin AL. Histologic characteristics of filtering blebs in glaucomatous eyes. *Arch Ophthalmol* 1983;101(5):795-798.

12 Schlunck G, Meyer-ter-Vehn T, Klink T, Grehn F. Conjunctival fibrosis following filtering glaucoma surgery. *Exp Eye Res* 2016;142:76-82.

13 Pimentel E, Schmidt J. Is mytomicyn better than 5-fluorouracil as antimetabolite in trabeculectomy for glaucoma? *Medwave* 2018;18(1):e7137.

14 Holló G. Wound healing and glaucoma surgery: modulating the scarring process with conventional antimetabolites and new molecules. *Dev Ophthalmol* 2017;59:80-89.

15 Cabourne E, Clarke JCK, Schlottmann PG, Evans JR. Mitomycin C versus 5-Fluorouracil for wound healing in glaucoma surgery. *Cochrane Database Syst Rev* 2015;2015(11):CD006259.

16 Tomasek JJ, Gabbiani G, Hinz B, Chaponnier C, Brown RA. Myofibroblasts and mechano-regulation of connective tissue remodelling. *Nat Rev Mol Cell Biol* 2002;3(5):349-363.

17 Gater R, Ipek T, Sadiq S, Nguyen D, Jones L, El Haj A, Yang Y. Investigation of conjunctival fibrosis response using a 3D glaucoma tenon's capsule + conjunctival model. *Invest Ophthalmol Vis Sci* 2019;60(2):605-614.

18 Pohlers D, Brenmoehl J, Löffler I, Müller CK, Leipner C, Schultze-Mosgau S, Stallmach A, Kinne RW, Wolf G. TGF-β and fibrosis in different organs—molecular pathway imprints. *Biochim Biophys Acta BBA Mol Basis Dis* 2009;1792(8):746-756.

19 Cordeiro MF. Role of transforming growth factor beta in conjunctival scarring. *Clin Sci* (*Lond*) 2003;104(2):181-187.

20 Freedman J. TGF-beta(2) antibody in trabeculectomy. *Ophthalmology* 2009;116(1):166.

21 Mead AL, Wong TTL, Cordeiro MF, Anderson IK, Khaw PT. Evaluation of anti-TGF-β2 antibody as a new postoperative anti-scarring agent in glaucoma surgery. *Invest Ophthalmol Vis Sci* 2003;44(8):3394.

22 Chytil A, Magnuson MA, Wright CV, Moses HL. Conditional inactivation of the TGF-beta type II receptor using Cre: Lox. *Genesis* 2002;32(2):73-75.

23 Inman GJ, Nicolás FJ, Callahan JF, Harling JD, Gaster LM, Reith AD, Laping NJ, Hill CS. SB-431542 is a potent and specific inhibitor of transforming growth factor-beta superfamily type I activin receptor-like kinase (ALK) receptors ALK4, ALK5, and ALK7. *Mol Pharmacol* 2002;62(1):65-74.

24 Tuerk C, Gold L. Systematic evolution of ligands by exponential enrichment: RNA ligands to bacteriophage T4 DNA polymerase. *Science* 1990;249(4968):505-510.

25 Ellington AD, Szostak JW. *In vitro* selection of RNA molecules that bind specific ligands. *Nature* 1990;346(6287):818-822.

26 Wu XQ, Liu HL, Han DM, Peng B, Zhang H, Zhang L, Li JL, Liu J, Cui C, Fang SB, Li M, Ye M, Tan WH. Elucidation and structural modeling of CD71 as a molecular target for cell-specific aptamer binding. *J Am Chem Soc* 2019;141(27):10760-10769.

27 He JQ, Wang JY, Zhang N, Shen LY, Wang LL, Xiao X, Wang Y, Bing T, Liu XJ, Li SQ, Shangguan DH. *In vitro* selection of DNA aptamers recognizing drug-resistant ovarian cancer by cell-SELEX. *Talanta* 2019;194:437-445.

28 Zhu XY, Li L, Zou LY, Zhu XD, Xian GJ, Li HJ, Tan Y, Xie L. A novel aptamer targeting TGF-β receptor II inhibits transdifferentiation of

human tenon's fibroblasts into myofibroblast. *Invest Ophthalmol Vis Sci* 2012;53(11):6897-6903.

29 Li XR, Leng Y, Li XJ, Wang YW, Luo P, Zhang C, Wang ZW, Yue XF, Shen CX, Chen L, Liu ZJ, Shi CM, Xie L. The TβR II-targeted aptamer S58 prevents fibrosis after glaucoma filtration surgery. *Aging* 2020;12(10):8837-8857.

30 Tatischeff I, Alfsen A. A new biological strategy for drug delivery: eucaryotic cell-derived nanovesicles. *J Biomater Nanobiotechnology* 2011;2(5):494-499.

31 Chauhan S, Danielson S, Clements V, Edwards N, Ostrand-Rosenberg S, Fenselau C. Surface glycoproteins of exosomes shed by myeloid-derived suppressor cells contribute to function. *J Proteome Res* 2017;16(1):238-246.

32 Zhang Y, Liu YF, Liu HY, Tang WH. Exosomes: biogenesis, biologic function and clinical potential. *Cell Biosci* 2019;9:19.

33 van den Boorn JG, Schlee M, Coch C, Hartmann G. SiRNA delivery with exosome nanoparticles. *Nat Biotechnol* 2011;29(4):325-326.

34 Alvarez-Erviti L, Seow Y, Yin HF, Betts C, Lakhal S, Wood MJA. Delivery of siRNA to the mouse brain by systemic injection of targeted exosomes. *Nat Biotechnol* 2011;29(4):341-345.

35 Sun Z, Wang L, Dong LH, Wang XJ. Emerging role of exosome signalling in maintaining cancer stem cell dynamic equilibrium. *J Cell Mol Med* 2018;22(8):3719-3728.

36 Tian Y, Gong MF, Hu YY, Liu HS, Zhang WQ, Zhang MM, Hu XX, Aubert D, Zhu SB, Wu LN, Yan XM. Quality and efficiency assessment of six extracellular vesicle isolation methods by nano-flow cytometry. *J Extracell Vesicles* 2020;9(1):1697028.

37 Tian Y, Ma L, Gong MF, Su GQ, Zhu SB, Zhang WQ, Wang S, Li ZB, Chen CX, Li LH, Wu LN, Yan XM. Protein profiling and sizing of extracellular vesicles from colorectal cancer patients via flow cytometry. *ACS Nano* 2018;12(1):671-680.

38 Pužar Dominkuš P, Stenovec M, Sitar S, Lasič E, Zorec R, Plemenitaš A, Žagar E, Kreft M, Lenassi M. PKH26 labeling of extracellular vesicles: Characterization and cellular internalization of contaminating PKH26 nanoparticles. *Biochim Biophys Acta Biomembr* 2018;1860(6):1350-1361.

39 Sherwood MB, Esson DW, Neelakantan A, Samuelson DA. A new model of glaucoma filtering surgery in the rat. *J Glaucoma* 2004;13(5):407-412.

40 Sleath B, Davis S, Sayner R, Carpenter DM, Johnson T, Blalock SJ, Robin AL. African American patient preferences for glaucoma education. *Optom Vis Sci* 2017;94(4):482-486.

41 Frangogiannis N. Transforming growth factor-β in tissue fibrosis. *J Exp Med* 2020;217(3):e20190103.

42 Adachi T, Nakamura Y. Aptamers: a review of their chemical properties and modifications for therapeutic application. *Molecules* 2019;24(23):4229.

43 Kaczmarek JC, Kowalski PS, Anderson DG. Advances in the delivery of RNA therapeutics: from concept to clinical reality. *Genome Med* 2017;9(1):60.

44 Yu AL, Shi H, Liu H, Bao ZS, Dai ML, Lin D, Lin DQ, Xu X, Li XY, Wang YQ. Mucoadhesive dexamethasone-glycol chitosan nanoparticles for ophthalmic drug delivery. *Int J Pharm* 2020;575:118943.

45 Huang Y, Tao Q, Hou DZ, Hu S, Tian SY, Chen YZ, Gui RY, Yang LL, Wang Y. A novel ion-exchange carrier based upon liposome-encapsulated montmorillonite for ophthalmic delivery of betaxolol hydrochloride. *Int J Nanomedicine* 2017;12:1731-1745.

46 Kotterman MA, Schaffer DV. Engineering adeno-associated viruses for clinical gene therapy. *Nat Rev Genet* 2014;15(7):445-451.

47 Pack DW, Hoffman AS, Pun S, Stayton PS. Design and development of polymers for gene delivery. *Nat Rev Drug Discov* 2005;4(7):581-593.

48 van der Meel R, Fens MHAM, Vader P, van Solinge WW, Eniola-Adefeso O, Schiffelers RM. Extracellular vesicles as drug delivery systems: lessons from the liposome field. *J Control Release* 2014;195:72-85.

49 Sercombe L, Veerati T, Moheimani F, Wu SY, Sood AK, Hua SS. Advances and challenges of liposome assisted drug delivery. *Front Pharmacol* 2015;6:286.

50 Deshpande PP, Biswas S, Torchilin VP. Current trends in the use of liposomes for tumor targeting. *Nanomedicine* (*Lond*) 2013;8(9):1509-1528.

51 Litzinger DC, Buiting AM, van Rooijen N, Huang L. Effect of liposome size on the circulation time and intraorgan distribution of amphipathic poly(ethylene glycol)-containing liposomes. *Biochim Biophys Acta* 1994;1190(1):99-107.

52 Antimisiaris SG, Mourtas S, Marazioti A. Exosomes and exosome-inspired vesicles for targeted drug delivery. *Pharmaceutics* 2018;10(4):E218.

53 Ha D, Yang NN, Nadithe V. Exosomes as therapeutic drug carriers and delivery vehicles across biological membranes: current perspectives and future challenges. *Acta Pharm Sin B* 2016;6(4):287-296.

54 Mathieu M, Martin-Jaular L, Lavieu G, Théry C. Specificities of secretion and uptake of exosomes and other extracellular vesicles for cell-to-cell communication. *Nat Cell Biol* 2019;21(1):9-17.

55 Bebelman MP, Smit MJ, Pegtel DM, Baglio SR. Biogenesis and function of extracellular vesicles in cancer. *Pharmacol Ther* 2018;188:1-11.

56 Li DL, Zhang JX, Liu ZJ, Gong YY, Zheng Z. Human umbilical cord mesenchymal stem cell-derived exosomal miR-27b attenuates subretinal fibrosis *via* suppressing epithelial-mesenchymal transition by targeting HOXC6. *Stem Cell Res Ther* 2021;12(1):24.

57 Guiot J, Cambier M, Boeckx A, Henket M, Nivelles O, Gester F, Louis E, Malaise M, Dequiedt F, Louis R, S truman I, Njock MS. Macrophage-derived exosomes attenuate fibrosis in airway epithelial cells through delivery of antifibrotic miR-142-3p. *Thorax* 2020;75(10):870-881.

58 Kang JY, Park H, Kim H, Mun D, Park H, Yun NR, Joung B. Human peripheral blood-derived exosomes for microRNA delivery. *Int J Mol Med* 2019;43(6):2319-2328.

59 Ren XX, Zhao Y, Xue FQ, Zheng Y, Huang HX, Wang W, Chang YC, Yang H, Zhang JL. Exosomal DNA aptamer targeting α-synuclein aggregates reduced neuropathological deficits in a mouse Parkinson's disease model. *Mol Ther Nucleic Acids* 2019;17:726-740.

60 Lamichhane TN, Jeyaram A, Patel DB, Parajuli B, Livingston NK, Arumugasaamy N, Schardt JS, Jay SM. Oncogene knockdown via active loading of small RNAs into extracellular vesicles by sonication. *Cell Mol Bioeng* 2016;9(3):315-324.

61 Melzer C, Rehn V, Yang YY, Bähre H, von der Ohe J, Hass R. Taxol-loaded MSC-derived exosomes provide a therapeutic vehicle to target metastatic breast cancer and other carcinoma cells. *Cancers* 2019;11(6):798.

62 van Dongen HM, Masoumi N, Witwer KW, Pegtel DM. Extracellular vesicles exploit viral entry routes for cargo delivery. *Microbiol Mol Biol Rev* 2016;80(2):369-386.

63 Millard M, Yakavets I, Piffoux M, Brun A, Gazeau F, Guigner JM, Jasniewski J, Lassalle HP, Wilhelm C, Bezdetnaya L. mTHPC-loaded extracellular vesicles outperform liposomal and free mTHPC formulations by an increased stability, drug delivery efficiency and cytotoxic effect in tridimensional model of tumors. *Drug Deliv* 2018;25(1):1790-1801.

64 Schindler C, Collinson A, Matthews C, Pointon A, Jenkinson L, Minter RR, Vaughan TJ, Tigue NJ. Exosomal delivery of doxorubicin enables rapid cell entry and enhanced *in vitro* potency. *PLoS One* 2019;14(3):e0214545.

65 Heusermann W, Hean J, Trojer D, Steib E, von Bueren S, Graff-Meyer A, Genoud C, Martin K, Pizzato N, Voshol J, Morrissey DV, Andaloussi SEL, Wood MJ, Meisner-Kober NC. Exosomes surf on filopodia to enter cells at endocytic hot spots, traffic within endosomes, and are targeted to the ER. *J Cell Biol* 2016;213(2):173-184.

66 Bissig C, Gruenberg J. ALIX and the multivesicular endosome: ALIX in wonderland. *Trends Cell Biol* 2014;24(1):19-25.